Relevance of Cooperative Lattice Effects and Stress Fields in Phase-Separation Theories for CMR Manganites

Jan Burgy, Adriana Moreo, and Elbio Dagotto

National High Magnetic Field Lab and Department of Physics, Florida State University, Tallahassee, Florida 32306, USA
(Received 26 June 2003; published 2 March 2004)

Previous theoretical investigations of colossal magnetoresistance (CMR) materials explain this effect using a "clustered" state with preformed ferromagnetic islands that rapidly align their moments with increasing external magnetic fields. While qualitatively successful, explicit calculations indicate drastically different typical resistivity values in two- and three-dimensional lattices, contrary to experimental observations. This conceptual bottleneck in the phase-separated CMR scenario is resolved here considering the *cooperative* nature of the Mn-oxide lattice distortions. This effectively induces power-law *correlations* in the quenched disorder used in toy models with phase competition. When these effects are incorporated, resistor-network calculations reveal very similar results in two and three dimensions, qualitatively modifying previous scenarios and solving the puzzle.

The study of self-organization in transition-metal oxides (TMO) is one of the dominant scientific themes of condensed matter physics (CMP). This phenomenon includes the intrinsically inhomogeneous states of colossal magnetoresistance (CMR) manganites [1,2] and underdoped high temperature superconductors [3]. In these compounds, the competition between different ordering tendencies leads to complexity: their properties change dramatically upon the application of relatively small perturbations. In Mn oxides, the cross fertilization between theoretical and experimental investigations has been remarkably fruitful, and at present the existence of mixed-phase tendencies in the CMR regime is widely accepted [4]. The emerging CMR picture is based on nanoscale clusters of competing phases [2,4–6]. With increasing magnetic fields, the clusters with ferromagnetic (FM) characteristics rapidly align their moments, leading to a percolative insulator-metal transition. Other compounds share similar phenomenology, and "clustered states" are emerging as a novel paradigm of CMP [7].

However, an important unresolved issue that confronts the phase-separation scenario for the CMR oxides concerns the *dimensionality dependence* of current theoretical descriptions. Resistor-network calculations in two dimensions (2D) reported a colossal MR effect, compatible with experiments, near the clean-limit low-temperature first-order FM-antiferromagnetic (AF) phase transition [4]. Disorder was further shown to smear the FM-AF transition region into a glassy clustered state [6]. Well-known arguments [8] predict that, in 2D, infinitesimal disorder is sufficient to create large coexisting clusters of neighboring phases. However, similar simulations in three dimensions (3D) (shown below) do not lead to equally impressive resistivity ρ vs temperature curves. Within the Imry-Ma reasoning [8] the critical dimension is 2, and only an unphysically large disorder strength Δ_c can destabilize the uniform 3D FM phase of the random

field Ising model (RFIM). Moreover, for $\Delta \gtrsim \Delta_c$ the resulting clusters are not large enough to induce a substantial ρ. Therefore, it is crucial to resolve this incorrect dimensional dependence. Since the phenomenology emerging from simulations in 2D matches qualitatively the experimental results gathered in *both* 2D and 3D, mixed-phase tendencies likely dominate in real materials. Moreover, experiments have unveiled a remarkable instability of the CE phase to the introduction of disorder in 3D, showing that disorder is by no means irrelevant in real perovskite manganites [9]. This is also compatible with recent small-clusters simulations [10,11]. Nevertheless, in the transition from realistic models, which cannot be simulated on large enough lattices for percolation, to the RFIM-like toy models that can successfully estimate magnetoresistances [6], an unphysical dimensionality dependence suggests a conceptual ingredient is missing.

In this Letter, the dimensionality-dependence puzzle is solved. The crucial issue unveiled here is the key relevance of *cooperative* effects and stress fields for quantitative magnetoresistance studies of Mn oxides. Cooperation introduces correlations in the quenched disorder needed to render percolative the clean-limit standard FM-AF first-order transition of simple models of phase competition. Previous simulations used uncorrelated disorder [6], and this induced the substantial quantitative differences between 2D and 3D. The disorder discussed here is inevitable—and, thus, intrinsic—in the standard chemical-doping process widely used to control the hole density, or average hopping amplitude, in TMO. Replacing trivalent by divalent ions of different sizes introduces MnO_6 octahedra distortions that cause local disorder. Once a distortion is created, it *propagates* following a power-law decay $1/r^\alpha$ governed by standard elasticity mechanisms that suggest $\alpha \sim 3$ (see Ref. [12]). This propagation emerges from the cooperative nature of the distortions, since adjacent MnO_6 octahedra share an

oxygen. Cooperation is crucial [13] to study charge-ordered states at fillings such as $x = 0.5$. The present effort shows that cooperation is also crucial for the understanding of the dimensionality dependence of CMR simulations.

The key relevance of cooperative effects can be dramatically illustrated via Monte Carlo (MC) simulations of the two-orbital double-exchange (DE) model coupled to Jahn-Teller (JT) classical phonons. The Hamiltonian and details of the simulations have been extensively described in previous literature [13]. The explicit use of oxygen degrees of freedom (d.o.f.) introduces cooperation in the distortions. To simplify the calculation and allow the study of 64-site clusters, the t_{2g} classical spins were frozen in a FM state and the transitions studied here involve only the charge/orbital d.o.f. This is not restrictive since recent studies [10] have unveiled charge/orbital order-disorder transitions at hole density $x = 0.5$ even with the spins in a FM configuration, by varying the electron-phonon coupling λ. The charge-ordered (CO) phase has the same arrangement of charge and orbitals as the realistic CE state [10,14]. Although the MC study in Fig. 1 is necessarily restricted to 2D, this is sufficient to show the key role of oxygen cooperation, illustrating the limitations in previous uncorrelated-disorder assumptions. Typical results in the $x = 0.5$ clean limit, and with λ larger than the critical value λ_c toward a CO state [10], reveal the familiar pattern of charge-diagonal stripes with $(3x^2\text{-}r^2/3y^2\text{-}r^2)$ populated orbitals [Fig. 1(a)]. This order is dramatically affected when, to simulate quenched disorder, the value of λ is made subcritical in four sites of the 64-site cluster [just ~6% of the sites, Fig. 1(b)]. The stripe pattern *disappears* and a random-looking distribution of charge and orbitals is stabilized, due to the nonlocal character of the disturbance caused by the four subcritical sites (compatible with recent simulations [10,11]). In Fig. 1(c), the situation is reversed: the background has a $\lambda < \lambda_c$ and, as a consequence, the lowest-energy state is not charge/orbital ordered in the clean limit. However, once four sites carry $\lambda > \lambda_c$, a stripelike pattern emerges, affecting most of the lattice. Finally, even at $x = 0$, having the four sites of a plaquette above λ_c—with the rest below λ_c(see Ref. [15])—is sufficient to induce a staggered pattern on the entire cluster [Fig. 1(d)]. These realistic-model simulations show that *cooperation dramatically enhances the role of quenched disorder in manganite models.*

The results in Fig. 1 indicate that it is inappropriate to use the RFIM with uncorrelated disorder to mimic the physics of Mn oxides. If a chemical-doping-induced lattice distortion at a Mn-Mn link leads to, e.g., a decrease of the hopping amplitudes, the neighboring links tend to have a similar reduction due to the slow power-law decrease of the elastic distortion. As a consequence, a proper RFIM modeling of real manganites requires a correlation in the random fields. More formally, consider the modified RFIM Hamiltonian $H = -J\sum_{\langle ij \rangle} s_i s_j -$
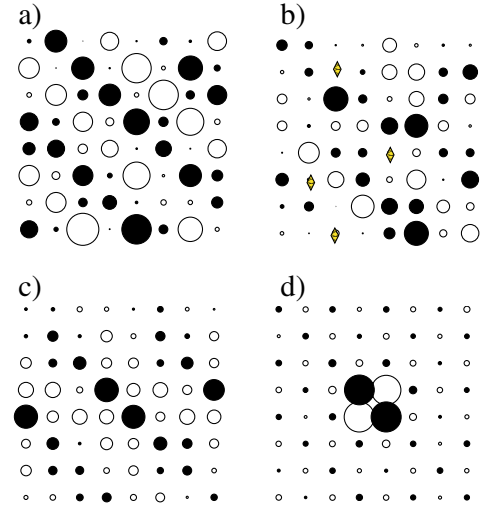

FIG. 1 (color online). MC results for the two-orbital DE model with cooperative JT phonons, on a 8×8 lattice at low temperature ($T = 0.01$, in hopping units). The Hund coupling is ∞, and the classical spins are assumed ferromagnetically aligned for simplicity. Cooperation is included by using the oxygen coordinates as d.o.f. Only the Q_2 mode is active (not a restrictive assumption, since at $x = 0$ and 0.5, Q_2 is the most relevant mode [2]). (a) Clean-limit results for $\lambda = 1.6 > \lambda_c = 1.4$, and $x = 0.5$. The filled and open circles indicate positive and negative $\langle Q_2 \rangle$, respectively, concomitant with populated orbitals oriented along the x and y axes. The $\langle Q_2 \rangle$ absolute value, proportional to the dot radius, is related to the charge at each site. The previously documented stripes [1,2,4] are observed in the simulation (the small deviations from a perfect arrangement are caused by finite-T effects). (b) Same as (a) but with four sites (diamonds) where $\lambda = 0.0$. Now the stripe pattern is drastically disrupted, showing the sensitivity of the CO state to disorder [10,11]. (c) Illustration of the opposite effect as in (a),(b): here λ is subcritical ($= 1.2$) everywhere but in the four sites with the largest dots where $\lambda = 2 > \lambda_c$. A clean-limit study with uniform $\lambda = 1.2$ reveals no order, but including just four sites with $\lambda > \lambda_c$ creates short-range stripe order. Here and in (d) the dot area is proportional to $\langle Q_2 \rangle$. (d) Similar to (c) but for $x = 0.0$. $\lambda = 0.4$ (below $\lambda_c = 0.5$) at all sites but the four with the largest dots, where $\lambda = 2.0$. The ordered plaquette generates charge ordering on the entire 64-site lattice.

$\Delta\sum_{i,j} h_i s_j / d_{ij}^\alpha$, where s_i are Ising variables, J is the FM coupling, Δ is the disorder strength, and d_{ij} is the distance between lattice sites i and j (in practice, d_{ij}^α was replaced by $(1 + d_{ij}^2)^{\alpha/2}$, with the same asymptotic behavior but remaining finite at zero distance). In this model, a ''random'' perturbation h_i at site i influences the neighboring dynamical variables s_j well beyond the usual on-site $i = j$ range, as the analysis in Fig. 1 indicates. By redefining, $\tilde{h}_j = \sum_i h_i / d_{ij}^\alpha$, the Hamiltonian can be cast in the standard form $H = -J\sum_{\langle ij \rangle} s_i s_j - \Delta\sum_j \tilde{h}_j s_j$, but now with *correlated disorder* since $\langle \tilde{h}_i \tilde{h}_j \rangle = 1/d_{ij}^{2\alpha-D}$ (D = lattice dimension). The critical value of α—below which the system breaks into domains for infinitesimal Δ—is $\alpha_c = (D/2) + 1$, which for $D = 3$ is $\alpha_c = 2.5$ (for

details, see Ref. [16], and references therein). The important point for our purposes is that correlated disorder can alter the critical dimension, and its value can be raised to 3 if $\alpha \leq 2.5$. To test these ideas, the Hamiltonian H has been studied using algorithms that allows for the direct calculation of RFIM ground states [17] (see Fig. 2). In agreement with our expectations, there is a dramatic qualitative difference between the results obtained with uncorrelated disorder ($\alpha = \infty$) and those obtained using a value of α ($\alpha = 3$) that more realistically mimics the elasticity. In particular, Fig. 2 shows that the former exhibits a large Δ_c and small clusters, while the latter has large clusters and a $\Delta_c \sim 10$ times smaller than the value obtained with uncorrelated disorder.

To further verify these ideas, the formalism already presented in Ref. [6] is here employed. To generate phase competition, a simple spin model with competing interactions is used $H = -J\sum_{\langle ij \rangle} s_i s_j + J'\sum_{[ik]} s_i s_k$, where s_i are Ising variables, and J (J') is a nearest-neighbors (next-nearest-neighbors) FM (AF) coupling. For small J'/J, the $T = 0$ dominant state is FM, while at large J'/J it has
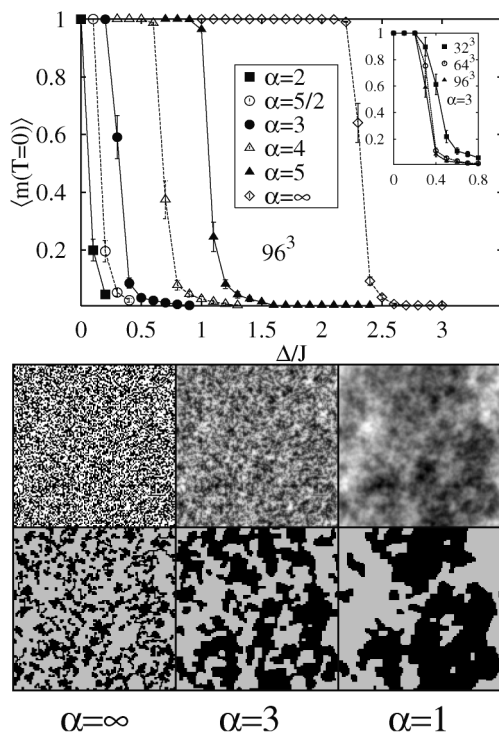
collinear AF features (alternating lines of spins up and down). The clean-limit critical value is $J'/J = 0.25$ (0.5) in 3D (2D). Disorder is introduced by the replacement $J' \rightarrow J'_{ik} = J' + W\tilde{\epsilon}_{ik}$ at every plaquette diagonal, with $\tilde{\epsilon}_{ik}$ being random numbers in $[1/2, -1/2]$ spatially *correlated* as $\tilde{h}_j$. Disorder reduces the values of the clean-limit critical temperatures T^* to T_C—as extensively discussed before [2,6]—creating an intermediate T region where FM clusters with random moment orientations are found. A grid of resistors can be constructed and the effective cluster resistance can be calculated, following standard procedures [6]. Results are in Fig. 3. Figure 3(a) shows the net resistivity ρ vs T, at several J's, with weak ($W \ll J$) disorder incorporated. For all J's, a fairly *sharp peak* is found between T_C and T^* for $\alpha = 3$, the exponent that mimics the effect of elastic forces. These ρ profiles are in good agreement with Mn-oxide experiments. Figure 3(b) illustrates the W dependence of the results. For sufficiently large W, the clusters are small and ρ is not enhanced at intermediate temperatures. As W is reduced, the clusters increase in size and the peak in ρ develops. Figure 3(c) contains ρ vs T, parametric with magnetic fields, for the case of *uncorrelated* disorder. In agreement with the introductory discussion, ρ here is 2 orders of magnitude *smaller* than with correlated disorder, illustrating the dramatic differences that correlated quenched disorder, mimicking stress fields, causes in the
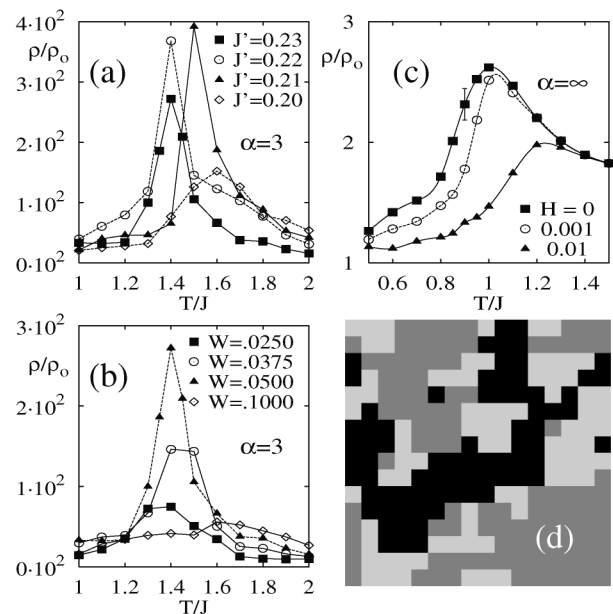

FIG. 2.   Top panel: computer-generated ground-state magnetization $\langle m(T = 0) \rangle$ of the RFIM vs Δ, for several values of the disorder correlation exponent. $\alpha = 2.5$ is the predicted 3D critical value below which infinitesimal disorder will destroy long-range order. Note the dramatic difference among the several αs. The inset shows $\langle m(T = 0) \rangle$ vs Δ for three different lattice sizes and $\alpha = 3$, to illustrate finite-size effects. Bottom panel: snapshots of a typical random field distribution $\tilde{h}_i$ (top row) and corresponding Ising spin configuration (bottom row), for three αs on a 128^2 lattice and $\Delta/J = 1$, to visualize cluster sizes and shapes. 2D clusters are used to access large linear sizes, but results are similar in 3D [see Fig. 3(c)] [18].

FIG. 3.   (a) J' dependence of ρ (in units of the metallic regions resistivity ρ_0) for the 3D J-J' model with long-range correlated disorder ($\alpha = 3$), at $W/J = 0.05$. (b) ρ dependence on the disorder strength W, at $J'/J = 0.23$. (c) ρ in 3D without long-range correlated disorder (i.e., at $\alpha = \infty$), much smaller than in (a),(b). (d) Slice of a 32^3 lattice at $T/J = 1.4$, $J'/J = 0.23$, and $W/J = 0.05$. Black and dark gray are FM regions with opposite orientations of their magnetic moments, and light gray are competing state (collinear AF) regions.
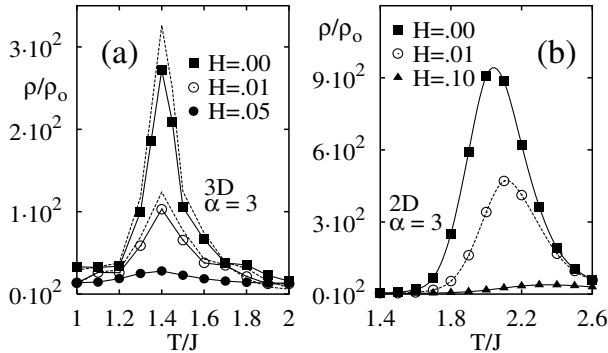
FIG. 4.　(a) ρ/ρ_0 vs T for the J-J' model ($J'/J = 0.23$ and $W/J = 0.05$) with long-range correlated disorder ($\alpha = 3$), in 3D and for the magnetic fields indicated. Solid (dashed) lines are results on 16^3 (32^3) lattices. (b) Same as (a), but on a 64^2 2D lattice, with $J'/J = 0.68$ and $W/J = 0.1$. Clearly, now both 2D and 3D results are quite similar in magnitude.

quantitative results. Finally, dominant MC configuration snapshots [Fig. 3(d)] reveal an intricate cluster arrangement in the T region of interest if $\alpha = 3$—far from the uniformly polarized state at the same W if $\alpha = \infty$—intuitively justifying the observed high ρ values [2,6]. The proximity of $\alpha = 3$ to $\alpha_c = 2.5$, and the anticipated further effective reduction of α if Coulombic disorder effects were incorporated, lead us to believe that the sub-μm clusters reported in Ref. [5] could indeed be intrinsic to Mn oxides. *It is the combination of phase competition and correlated disorder that creates the CMR behavior in our 3D toy model.* The effect substantially decreases away from the phase competition region, even though the correlation in disorder remains always "on."

Although the previous results show that disorder-correlation effects are important, only a magnetoresistance estimation can clarify its role in the CMR effect itself. For this purpose, Fig. 4 contains a 3D/2D resistor-network calculation of ρ, with correlated disorder, varying the magnetic field. The peak in the resistivity—between T_C and T^*—is clear and has a *similar value* in both 3D and 2D. This is a considerable improvement over results with uncorrelated disorder, where the peak resistivity ratios between 2D and 3D are as high as 200 or more [see Ref. [6] and Fig. 3(c)]. The effect of small magnetic fields—that effectively "rotate" preformed FM clusters—is now strong in both dimensions of interest, and colossal MR ratios are obtained with minimal tuning of couplings (Fig. 4).

Summarizing, explicit calculations in toy models for the CMR phenomenon show that the critical dimension of the system is altered by disorder correlation, and when elasticity effects are included magnetoresistance ratios of comparable magnitude are obtained in 2D and 3D. These results are qualitatively different from previous investigations and remove a conceptual roadblock of phase-separation-based theoretical studies of manganites by demonstrating the importance of cooperative effects, reaffirming the potential relevance of clustered states in the description of TMO.

[1] *Colossal Magnetoresistance Oxides*, edited by Y. Tokura (Gordon & Breach, New York, 2000).

[2] E. Dagotto, *Nanoscale Phase-Separation and Colossal Magnetoresistance* (Springer-Verlag, Berlin, 2002).

[3] S. H. Pan *et al.*, Nature (London) **413**, 282 (2001); J. M. Tranquada *et al.*, Nature (London) **375**, 561 (1995).

[4] E. Dagotto *et al.*, Phys. Rep. **344**, 1 (2001).

[5] M. Uehara *et al.*, Nature (London) **399**, 560 (1999); J. Lynn *et al.*, Phys. Rev. Lett. **76**, 4046 (1996) and J. De Teresa *et al.*, Nature (London) **386**, 256 (1997); P. G. Radaelli *et al.*, Phys. Rev. B **63**, 172419 (2001); D. N. Argyriou *et al.*, Phys. Rev. Lett. **89**, 036401 (2002).

[6] J. Burgy *et al.*, Phys. Rev. Lett. **87**, 277202 (2001).

[7] H. Rho *et al.*, Phys. Rev. Lett. **88**, 127401 (2002); C. S. Snow *et al.*, Phys. Rev. Lett. **89**, 226401 (2002); G. Alvarez *et al.*, Phys. Rev. Lett. **89**, 277202 (2002).

[8] Y. Imry and S. K. Ma, Phys. Rev. Lett. **35**, 1399 (1975); J. F. Fernandez *et al.*, Phys. Rev. Lett. **51**, 203 (1983).

[9] D. Akahoshi *et al.*, Phys. Rev. Lett. **90**, 177203 (2003).

[10] H. Aliaga *et al.*, Phys. Rev. B **68**, 104405 (2003).

[11] Y. Motome *et al.*, Phys. Rev. Lett. **91**, 167204 (2003).

[12] D. I. Khomskii and K. I. Kugel, Europhys. Lett. **55**, 208 (2001); Phys. Rev. B **67**, 134401 (2003). Anisotropies in the strain fields are not included in our calculation. Elastic effects have also been discussed in A. R. Bishop *et al.*, Europhys. Lett. **63**, 289 (2003); K. H. Ahn *et al.*, Phys. Rev. B **68**, 092101 (2003); A. Bussmann-Holder and A. R. Bishop, Phys. Rev. B **56**, 5297 (1997); S. Semenovskaya and A. G. Khachaturyan, Phys. Rev. Lett. **67**, 2223 (1991), and references therein; H. Ahn and A. Millis, Phys. Rev. B **64**, 115103 (2001). The effect of long-range Coulomb interactions near first-order transitions has also been recently investigated: Kun Yang, Phys. Rev. B **67**, 092201 (2003).

[13] T. Hotta *et al.*, Phys. Rev. B **60**, R15 009 (1999); S. Yunoki *et al.*, Phys. Rev. Lett. **84**, 3714 (2000); see also J. A. Verges *et al.*, Phys. Rev. Lett. **88**, 136401 (2002).

[14] T. Hotta *et al.*, Phys. Rev. Lett. **86**, 4922 (2001).

[15] T. Hotta *et al.*, Phys. Rev. Lett. **90**, 247203 (2003).

[16] T. Nattermann, J. Phys. C **16**, 6407 (1983).

[17] A. Goldberg and R. Tarjan, J. Assoc. Comput. Mach. **35**, 921 (1988), and references therein.

[18] Note the close similarities of the cluster shapes with those investigated in J. Burgy *et al.*, Phys. Rev. B **67**, 014410 (2003) and D. Khomskii and L. Khomskii, Phys. Rev. B **67**, 052406 (2003).